JOURNAL OF SPACECRAFT AND ROCKETS
Vol. 40, No. 5, September–October 2003
This paper reprinted from AIAA Journal, Vol. 4, No. 12, 1966, pp. 2136–2141

A Time-Dependent Computational Method for Blunt Body Flows

GINO MORETTI* AND MICHAEL ABBETT†
General Applied Science Laboratories Inc., Westbury, N. Y.

The steady blunt body problem is solved using a time-dependent technique. The steady solution is reached asymptotically. The computation is performed in the shock layer only, assuming that the shock wave is a discontinuity surface, dependent on time. A technique similar to the one used by Richtmyer, Lax, and Wendroff is applied to the points between shock and body, whereas the shock and body points are analyzed with a three-dimensional method of characteristics. In this way a coarse mesh can be used, and little time is needed on the computer to achieve accurate results. Detailed results for two-dimensional (symmetric and asymmetric) blunt bodies and for axisymmetric ones are given and compared with experimental data. A brief critical comparison of the present technique with other methods also is given.

Nomenclature

a = speed of sound
b = abscissa of the body in the x, y plane
g = dummy variable
M = Mach number
p = pressure (divided by freestream pressure)
P = $\ln p$
R = $\ln \rho$
s = abscissa of the shock in the x, y plane
S = nondimensional entropy $S = P - \gamma R$
S_{sl} = nondimensional entropy behind a steady normal shock
t = nondimensional time in physical coordinate system
T = nondimensional time in transformed coordinate system
u = nondimensional velocity in x direction in x, y plane
U = nondimensional velocity in ξ direction in ξ, η plane
v = nondimensional velocity in y direction in x, y plane
V = nondimensional velocity in η direction in ξ, η plane
W = velocity of the shock in x direction in x, y plane
x = abscissa in a Cartesian frame in the physical plane
y = ordinate in a Cartesian frame in the physical plane
Y = ordinate in a Cartesian frame in the transformed plane
γ = ratio of specific heats
δ = $s - b$
ζ = abscissa in a Cartesian reference frame in the transformed plane
ξ, η = Cartesian reference frame along shock or body
θ = angle between tangent to shock and x axis
ρ = density (divided by freestream density)
φ = angle between tangent to body and x axis

Introduction

A TECHNIQUE for solving the well-known "blunt body problem"[1] is presented, having four important features, namely: 1) it is a direct method in the sense that the body geometry is prescribed and controls the subsequent computation; 2) it can provide results as accurate as needed, and control of accuracy is achieved by a simple change in the input data, not by a reformulation of the analysis; 3) it requires a relatively short time on a high speed computer (down to a minimum of a few seconds) if a coarse mesh is used, but even the coarsest mesh is sufficient to achieve surprisingly accurate results; and 4) it is not restricted to a simplified thermodynamical model.

Choice of a Technique

Many solutions for this problem have been proposed in the past. A discussion of their relative merits and disadvantages has been given in Ref. 3. Briefly, techniques that transform the mixed problem into a hyperbolic one[7–11] have been judged as being preferable to inverse methods using either marching techniques[5] or series expansions[4,6] and to strip methods.[2] However, Garabedian's[7] still is an inverse technique and the existing time-dependent methods[8] have some shortcomings that restrict their use for practical purposes. The basic idea of time-dependent techniques, as suggested by von Neumann,[10] is to consider the unsteady flow equations and to follow the evolution of the flow in time until it settles down to a steady pattern. The storage required is extremely large, and the computational time is too lengthy as a result of the shock not being considered as a sharp discontinuity. In addition, some objections could be raised to the manner in which the boundary conditions on a rigid wall are handled.

J. von Neumann's idea has been analyzed and developed by Lax, Wendroff, and others.[11] By properly setting the equations into finite difference form, solutions may be obtained in which shock waves are approximated by narrow regions where the physical parameters undergo sharp changes. Interesting as it may be from a theoretical standpoint (for the analysis of the relationship between the Rankine-Hugoniot equations and the Euler equations in conservation form, and for the analysis of artificial viscosity effects, etc.), such a technique is not necessarily the best approach to problems of steady flows such as the present one.

As an example, the reader is referred to recent computations by Bohachevski et al.[8] For the two-dimensional prob-

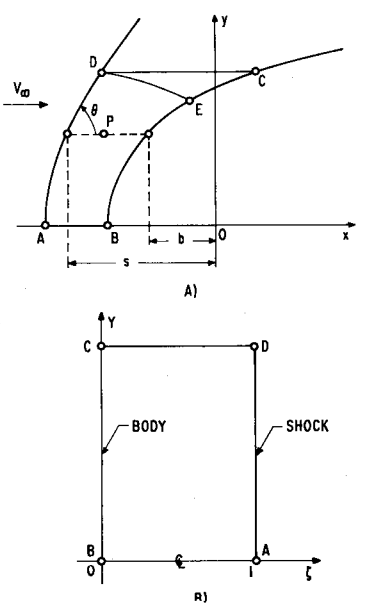

Fig. 1 Physical and transformed plane.

Received February 24, 1966; revision received July 13, 1966. This research is sponsored by the Advanced Research Projects Agency.

* Scientific Supervisor. Associate Fellow AIAA.

† Senior Scientist.

lem of the flow around a "step," a mesh of 3588 points was used, and the computation was carried along for 650 steps. The total running time on an IBM 7094 can be estimated as about 4 hr. However, it is evident from Figs. 2, 3, and 4 in the aforementioned paper that a steady state had not been reached when the computation was halted and that the shock is far from appearing as a distinct discontinuity.

One can easily see the advantages in assuming the shock wave as a discontinuity. First of all, no point need be computed in front of it. Second, the mesh in the shock layer may be kept rather coarse since the flow parameters are smooth functions of the space variables. In addition, the shock as a discontinuity seems to be more realistic than one several mesh sizes thick. In the present approach, therefore, a reduced number of points are computed in the region between shock and body, in the spirit of von Neumann, and a procedure is provided for describing the shock wave as a discontinuity and for following its motion. The technique will be described in some detail for the two-dimensional symmetric problem, the gas being treated as perfect, with a constant γ, and results will be given also for other cases.

Description of the Technique

Inner Points

Let Oxy (Fig. 1a) be a Cartesian frame of reference in the plane of motion. The body BC is assumed as symmetric with respect to the x axis. The flow at infinity is uniform, supersonic, and parallel to the x axis. The computation is performed in the region bounded by the line $ABCD$ where CD is parallel to the x axis; AD is an arc of the (still unknown) shock wave; and the location of C is chosen high enough to be sure that the flow, at any step of the computation, will be supersonic along CD.

The abscissa of the body b is a prescribed function of y and the abscissa of the shock wave s is a function of y and of time t. Let $\delta = s - b$. The angle between the shock wave and the x axis is called θ. Obviously, $\cot\theta = s_y$ (partial derivatives are indicated by subscripts). The partial derivative of s, with respect to t, will be called W; $W = s_t$ and may be interpreted as the x component of the local velocity of the shock wave.

An auxiliary set of independent variables ζ, Y, T, is introduced,

$$\zeta = (x - b)/\delta \qquad Y = y \qquad T = t$$

In the (ζ, Y) plane, the rectangle $ABCD$ of Fig. 1b is the counterpart of region $ABCD$ of Fig. 1a.

For any function $g(x, y, t)$,

$$g_x = g_\zeta/\delta \qquad g_y = g_Y + Cg_\zeta/\delta$$
$$g_t = g_T - W\zeta g_\zeta/\delta$$

where

$$C = (db/dy)(\zeta - 1) - \zeta\cot\theta$$

The equations of motion in the (ζ, Y, T) space are

$$\begin{aligned} R_T + BR_\zeta + vR_Y + u_\zeta/\delta + v_Y + Cv_\zeta/\delta &= 0 \\ u_T + Bu_\zeta + vu_Y + (p/\rho\delta)P_\zeta &= 0 \\ v_T + Bv_\zeta + vv_Y + (p/\rho)P_Y + (pC/\rho\delta)P_\zeta &= 0 \\ S_T + BS_\zeta + vS_Y &= 0 \end{aligned} \tag{1}$$

where p is the pressure, ρ is the density (divided by the pressure and density in the freestream, respectively), u and v are the x and y components of the velocity vector,

$$P = \ln p \qquad R = \ln\rho \qquad S = P - \gamma R$$
$$B = (u - W\zeta + vC)/\delta$$

Introducing P and R in place of p and ρ results in a simplification of the equations. The Cartesian frame in the physical plane has been used to simplify the analysis, although in principle any other frame could be used. However, the introduction of a rectangular mesh, as in Fig. 1b, is important for simplifying the numerical analysis.

To solve the equations of motion inside the rectangle of Fig. 1b, but not on the boundaries AD, DC, and CB, the value of any function g (g standing for R, u, v, S in turn) at a time $T + \Delta T$ is computed in the style of Wendroff by

$$g(T + \Delta T) = g(T) + g_T(T)\Delta T + g_{TT}(T)[\Delta T]^2/2 \tag{2}$$

The first derivatives g_T are obtained directly from Eqs. (1). The second derivatives g_{TT} are obtained by differentiating Eqs. (1) with respect to ζ, Y, and T and then rearranging the terms. The first and second space derivatives are computed by finite differences

$$\begin{aligned} g_\zeta^{(n,m)} &= [g^{(n+1,\,m)} - g^{(n-1,\,m)}]/2\Delta\zeta \\ g_Y^{(n,\,m)} &= [g^{(n,\,m+1)} - g^{(n,\,m-1)}]/2\Delta Y \\ g_{\zeta\zeta}^{(n,\,m)} &= [g^{(n+1,\,m)} + g^{(n-1,\,m)} - 2g^{(n,\,m)}]/(\Delta\zeta)^2 \\ g_{YY}^{(n,\,m)} &= [g^{(n,\,m+1)} + g^{(n,\,m-1)} - 2g^{(n,\,m)}]/(\Delta Y)^2 \\ g_{Y\zeta}^{(n,\,m)} &= [g^{(n+1,\,m+1)} - g^{(n+1,\,m-1)} - g^{(n-1,\,m+1)} + \\ &\qquad g^{(n-1,\,m-1)}]/4\Delta Y\Delta\zeta \end{aligned} \tag{3}$$

where n refers to the ζ coordinate and m to the Y coordinate. The quantities R, P, u, and v are stored in the computer as double arrays (functions of Y and ζ). Their first and second derivatives then are computed easily, applying Eqs. (3) at each point inside the rectangle of Fig. 1b. Single arrays contain the values of db/dy, $\cot\theta$, s, b, W, and δ as functions of Y. B and C then can be obtained, as well as the other terms: δ_Y $(= \cot\theta - db/dy)$, W_Y, C_Y, B_Y, $C_\zeta(= -\delta_Y)$, and B_ζ, which are generated in differentiating Eqs. (1). There are a few more terms to be evaluated, namely δ_T, W_T, C_T, and B_T. Now, $\delta_T = s_T = W$, and $C_T = -\zeta d(\cot\theta)/dT = -\zeta s_{YT} = -\zeta W_Y$. The term W_T is computed as

$$W_T = [W(T + \Delta T) - W(T)]/\Delta T$$

To this effect, the shock values must be evaluated at the beginning of each step in time and the values of $W(T + \Delta T)$ as a function of Y must be stored in a special array. Having W_T, the computation of B_T is straightforward.

The computation previously described is stable if the Courant-Friedrichs-Lewy criterion[12] is satisfied; therefore, at each step a safe (stable) stepsize ΔT is evaluated as the minimum of $\Delta/1.5a(M + 1)$, where Δ is the smallest interval between ΔY and Δx, a is the speed of sound, and M is the Mach number. Symmetry conditions are imposed on the centerline BA.

Shock Points

The points on the boundary $ADCB$ are computed differently. We study the shock points first. To understand the philosophy of the approach, let us consider the problem of a one-dimensional unsteady flow with a shock wave penetrating into a uniform medium, region 1 (Fig. 2). Suppose that the flow is known at all the values of x at $t = t_0$, and that the location and the velocity of the shock wave are to be evaluated at $t = t_1 = t_0 + \Delta t$, together with the conditions behind the shock. Starting at Q_0 with a given slope of the shock, the approximate location of Q_1 may be found. A characteristic, defined by $dx/dt = u - a$, then is drawn backward from Q_1, and the compatibility equation is integrated along it, starting at P.

The matching of the values obtained from the Rankine-Hugoniot equations for a moving shock and of the values obtained from the compatibility equation provides the velocity of the shock at Q_1, together with the rest of the unknowns.

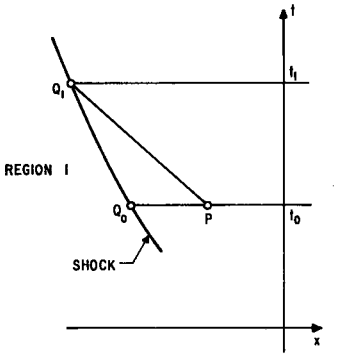

Fig. 2 Shock point in one-dimensional unsteady flow.

Obviously, the problem is to be solved by iteration, in the course of which some averaging of values between Q_1 and P may be made, and the location of Q_1 may be improved slightly.

The same technique may be used in the present problem, with an extension suggested by the procedure successfully used in computing three-dimensional steady flows.[13,14] Consider Fig. 3, where point Q_1 is the point on the shock wave at which the values are to be calculated at time $t_0 + \Delta t$ and Q is the point on the shock wave at time t_0, having the same y. A fixed Cartesian orthogonal frame $Q_0\,\xi\eta$ is defined, whose η axis is tangent to the shock wave at Q_1. Let U and V be the ξ and η components of the velocity vector at any point P. The equations of motion in the (ξ, η, t) space are

$$\begin{aligned} R_t + UR_\xi + U_\xi &= -VR_\eta - V_\eta \\ U_t + UU_\xi + (p/\rho)S_\xi + (\gamma p/\rho)R_\xi &= -VU_\eta \\ S_t + US_\xi &= -VS_\eta \\ V_t + UV_\xi &= -VV_\eta - (p/\rho)P_\eta \end{aligned} \tag{4}$$

It is well known that the η component of the velocity is the same on both sides of the shock. If a rigid motion defined by such a velocity, but in the negative direction of the η axis, is superimposed to the flowfield, the values of V then become very small. The right-hand sides of Eqs. (4) would actually vanish if the shock were rectilinear, though oblique. It thus is evident that, in the neighborhood of a shock point, the relevant parameters are ξ and U. Consequently, we consider the first three equations as quasi-one-dimensional equations, modified by forcing terms in the right-hand sides. From these three equations three characteristics are found in the (ξ, t) plane. They are defined by

$$d\xi/dt = U - a \qquad d\xi/dt = U + a \qquad d\xi/dt = U$$

and have immediate interpretation in terms of a quasi-one-dimensional flow. The compatibility equation along the first of these characteristics reads

$$[(a/\gamma)(dP/dt)] - (dU/dt) = -[(a/\gamma)VP_\eta + aV_\eta - VU_\eta] \tag{5}$$

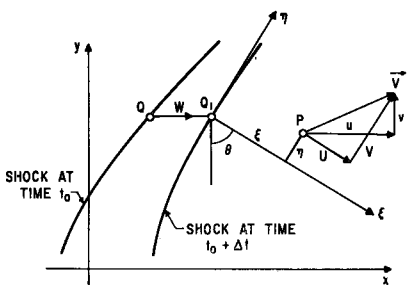

Fig. 3 Shock point in two-dimensional unsteady flow.

Table 1 Cases studied

Case	A	B	C	D
n^a =	2	3	5	7
m^b =	4	6	10	14

[a] Number of intervals in the x direction.
[b] Number of intervals in the y direction.

At a point on the shock, the Rankine-Hugoniot equations are:

$$U = \frac{(\gamma - 1)(V_\infty - W)^2 \sin^2\theta + 2a_\infty^2}{(\gamma + 1)(V_\infty - W)\sin\theta} + W\sin\theta \tag{6}$$

$$p = [2(V_\infty - W)^2 \sin^2\theta - (\gamma - 1)]/(\gamma + 1) \tag{7}$$

$$\rho = [(\gamma + 1)p + (\gamma - 1)]/[(\gamma + 1) + (\gamma - 1)p] \tag{8}$$

$$V = V_\infty \cos\theta \tag{9}$$

Equations (5–9) determine the solution at a shock point, including the local velocity of the shock wave W. The system is solved numerically by iteration. In this process, the location of point Q_1 and the corresponding value of θ are computed initially from the shape of the shock and the values of W at the previous step, and then are kept constant. From an assumed W, the values of U, p, and ρ are computed at the shock from Eqs. (6–8). A characteristic with the slope $d\xi/dt = U - a$ is drawn from point Q_1 in the (ξ, t) plane (Fig. 4), and its intersection A with the ξ axis is found. Since point A lies in the (x, y) plane at time t_0, and the solution is known completely at this time, local values of U and a are found at A by interpolating from the values at the mesh points in the (ζ, Y) plane at time $T = T_0$. A new characteristic then is issued from Q_1, with the slope $d\xi/dt = [(U - a)_{\text{shock}} + (U - a)_A]/2$, and the process is iterated until the location of point A is stabilized. At this stage, the right-hand side of Eq. (5) is computed at A and at Q_1, averaged, and considered constant between A and Q_1. Equation (5) can be integrated, assuming that P at the shock is the one obtained from (7), and a new value of U at the shock is computed. If it does not agree with the value obtained from (6), W is changed and the process repeated from the start. A trial-and-error technique then is used to achieve convergence on W.

Body Points

A similar computation is performed at the body points. The auxiliary frame of reference now is normal and tangent to the body. The characteristic having the slope $d\xi/dt = U + a$ is used to determine the pressure on the body since the ξ component of the velocity vanishes on it. The equation that determines the η component of the velocity [the last of (4)] is simplified, since $U = 0$, $v = V\sin\varphi$, and $g_\eta = g_Y \sin\varphi$, where φ is the angle between the tangent to the body and the x axis. It can be used in the form

$$V_t = -vV_Y - (p/\rho)P_Y \sin\varphi \tag{10}$$

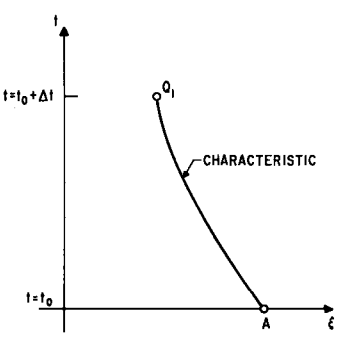

Fig. 4 One-dimensional characteristic.

The third of Eqs. (4) also is simplified into

$$S_t = -vS_Y \tag{11}$$

The whole computation is simpler than its counterpart on the shock, since the body wall is fixed.

Points on the Upper Boundary

The values of P, R, u, and v at points on the upper boundary CD merely are extrapolated linearly from the values computed inside; such a shortcut is justified. In reaching the steady state the upper region is supersonic. The downrunning characteristic issued from D (the DE line in Fig. 1a) is a frontier line across which no perturbations can be sent downward from the points above it. The region $ABED$ is insensitive to the technique by which the DC line is computed, and the only requirement is that along such a line values are used that do not generate local instability.

Initial Values

In principle, any set of initial values can be chosen. In order to provide a smooth computation, it is convenient to start with initial values that are distributed smoothly. An initial shape of the shock is taken, for example, a parabola. The shock is assumed to be initially at rest and the values behind it are computed. The initial pressure and density at the stagnation point are assumed to be the stagnation values behind a normal shock. The Mach number at point C on the body is assumed to be larger than one. The entropy along the body is assumed as constant. Velocity and density along the body are computed accordingly; a tentative value of the standoff distance is evaluated as a function of the curvature of the shock and the velocity distribution on the body; and the values of p, ρ, u, and v are interpolated smoothly between the shock and the body.

Analysis of Some Results

The analysis of the results is performed by studying the following data as functions of time: 1) the shape of the shock and, particularly, the standoff distance; 2) the velocity of each shock point (which should be zero under steady conditions); 3) the shape of the sonic line and, particularly, the y coordinate of the sonic points on the body and on the shock; 4) the pressure at the stagnation point (whose value is known in a steady state); and 5) the entropy on the centerline (whose value is also known in a steady state). A typical body was considered: an arc of a circle with unit radius followed by a straight line with a slope of 0.25 on the x axis. The computation was performed between $y = 0$ and $y = 2$. For $M_\infty = 4$, $\gamma = 1.4$, four meshes were used. Table 1 cites the

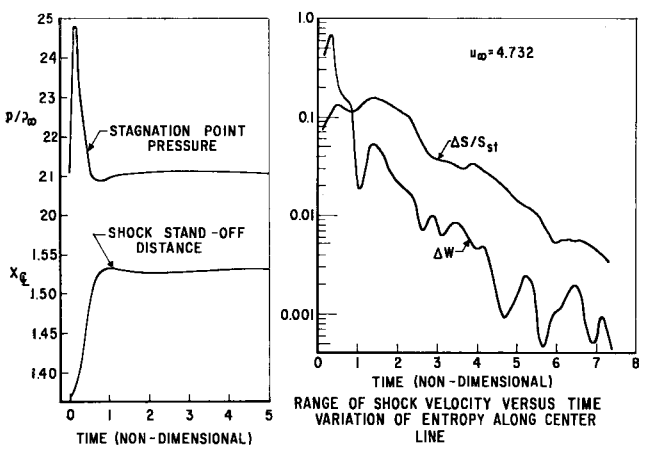

Fig. 5 Case C.

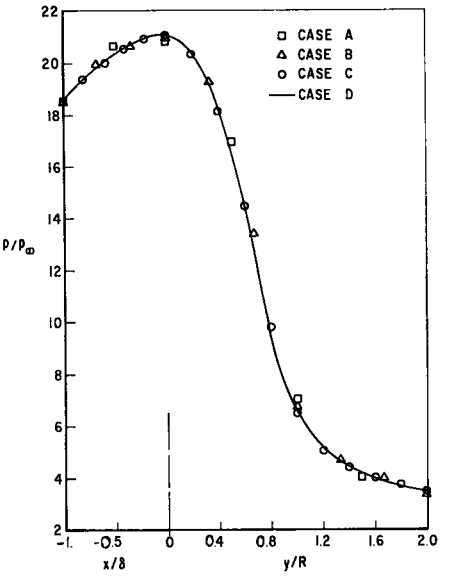

Fig. 6 Pressure along centerline from shock to body and along body for various mesh sizes.

cases studied if n is the number of intervals in the x direction, and m is the number of intervals in the y direction.

In Fig. 5 some significant results for case C are shown. The abscissa of the shock point on the centerline, the pressure at the stagnation point, the difference ΔW between the maximum and minimum values of the velocities of shock points, and the percent scattering of S on the centerline are plotted as functions of time. The tendency of the flowfield to settle down to a steady state is evident in all plots.

Figure 6 shows the pressure distribution between shock and body on the centerline and along the body for the four cases, A, B, C, and D. Figure 7 shows the stagnation pressure, the ordinate of the sonic point on the body and the shock, the standoff distance, and the abscissa of the upper point on the shock, as functions of the mesh size. It is evident that the accuracy is improved with decreasing mesh size and, on the other hand, that the asymptotic values are reached with meshes that are still very coarse. It also is evident that, for all practical purposes, even the 3×6 mesh of case B is sufficient. Statements 2 and 3 of the introduction then are justified. Table 2 cites the total running

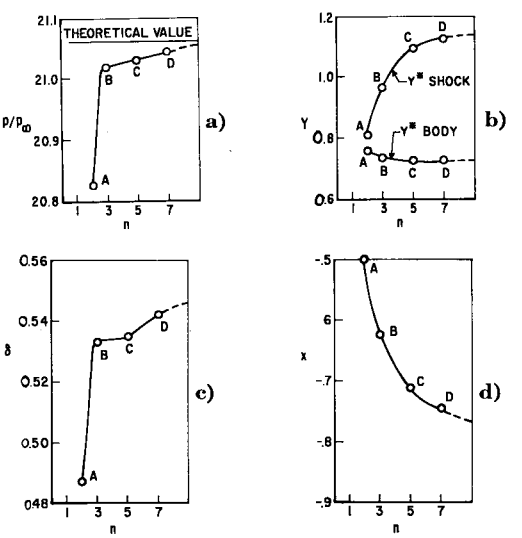

Fig. 7 a) Stagnation point pressure; b) location of sonic points on shock and body; c) shock stand-off distance; d) abscissa of upper point on shock.

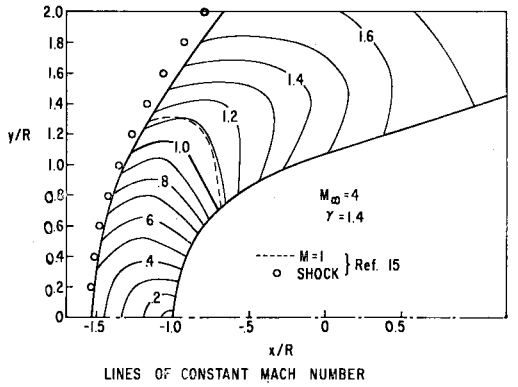

Fig. 8 Two-dimensional circular cylinder case D.

times for the four cases on an IBM 7094. In Fig. 8,‡ the shock shape, as obtained in case D, has been plotted together with a set of M = const lines. Dots and dotted lines in this figure are our best reproduction of the shock wave and the sonic line from the analysis of Belotserkovskii.[15]

It also is interesting to note that the initial distribution of values does not affect the asymptotic results. Several runs actually have been made with different initial conditions to prove this point. Consequently, in a final version of the program, a better choice of initial values was used, which gave a further reduction in running time.

In addition, a program that computes a steady supersonic flow starting at a down-running characteristic slightly above the sonic line was added. The asymptotic pressure distribution on the *CD* line of Fig. 1a computed with the present technique and the pressure distribution of the steady supersonic flow agree perfectly.

Two-Dimensional Asymmetric Blunt Body

No significant complications are introduced by considering two-dimensional asymmetric flows, since the basic logic of the technique is the same as for the symmetric case and the program is basically the same, except that the computation is performed over a wider region and no symmetry condition is imposed. Typical results are given in Ref. 3.

Axisymmetric Blunt Bodies

With minor changes in the coding of the symmetric two-dimensional program, consequent to the usage of a cylindrical frame instead of a Cartesian one, a program for computing axisymmetric blunt bodies was obtained. A sphere followed by a cone was considered first (its cross section with a meridional plane being the same as for the body of Fig. 8). A 5×10 mesh was used for $M_\infty = 4$, and a slightly wider region was computed for $M_\infty = 2$. The results [shock shape and M = const lines] are shown in Fig. 9.

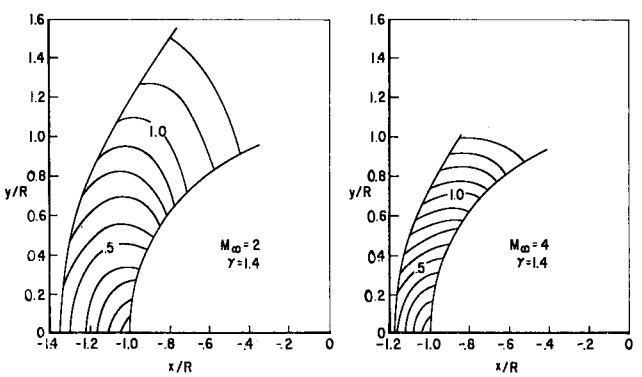

Fig. 9 Hemisphere-lines of constant Mach number.

‡ In figures that are partially reproduced from other sources, the original notation has been kept. Thus, in Figs. 8 and 12, R is the radius of the sphere and in Fig. 12, z is the axial coordinate.

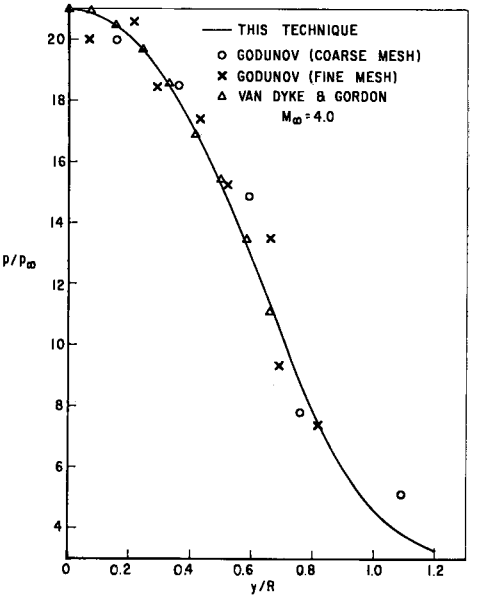

Fig. 10 Comparison of body pressure for hemisphere.

A detailed comparison of the present results with those obtained by Godunov et al.[9] using a technique that has in common with ours the idea of using a moving shock as one of the boundaries of the computed region, is given in Ref. 3. It seems quite clear that the technique discussed herein is more accurate than Godunov's and that the former can be extended more readily to cases with complicated thermodynamics, viscous effects, and three-dimensional flows. For example, Fig. 10 shows a comparison of body pressure values for the two techniques. In the same figure, values obtained by Van Dyke and Gordon[19] also are plotted.

Some time ago several agencies were asked by the Office of Naval Research (ONR) to provide their own results on the problem of an ellipsoid of revolution (with a 1:2 ratio of the axes) in a stream at $M_\infty = 3$, $\gamma = 1.4$. The results were collected and analyzed[16] and showed a regrettable scatter. We ran the same problem using two mesh sizes, one of 5×12, the other of 10×24 intervals. No appreciable changes were found between the two meshes. Figure 11 shows our values

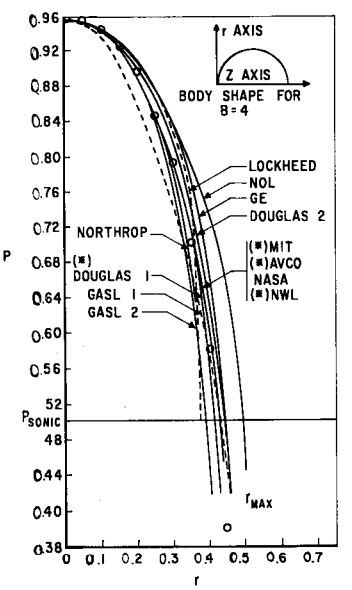

Fig. 11 Normalized body pressure P vs r.

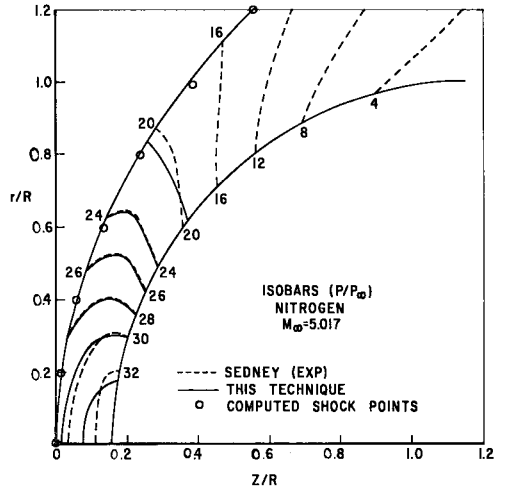

Fig. 12 Hemisphere-comparison of theory and experiment.

for the pressure distribution on the body as dots superposed on the original figure obtained at ONR.

Finally, Fig. 12 shows the isobars obtained experimentally by Sedney and Kahl[17] for a sphere in a nitrogen flow at $M_\infty = 5.017$. The shock wave obtained from experiments is drawn as a solid line. The other experimental lines are the dotted ones. Our computed points on the shock are the dots, and the computed isobars are the solid lines (some of them fit the dotted lines so well that the latter are not visible). This comparison is very satisfactory since our results have been obtained with a rather coarse mesh (as many lines in the y direction as dots on the shock of Fig. 12).

Physical Time vs Computed Time in an Unsteady Process

Assume that at $t = 0$ there exists a flowfield in front of the blunt body equal to the initial one in our computations. The steady state would be reached after a certain time t_1. The steady state is reached numerically after a number of steps, which amounts to a nondimensional total time T. The corresponding physical time t_2, is obtained by multiplying T by $r_0(\rho_\infty/p_\infty)^{1/2}$, where r_0 is that physical length assumed equal to one in the program. If t_2 is close enough to t_1, the computation can be considered as representing realistically an actual unsteady motion.

Unfortunately, no precise statement can be made at this time for lack of experimental evidence. The only available data, to our knowledge, have been obtained from experiments made with a very blunt body in a shock tube.[18] We will merely attempt an evaluation of orders of magnitude, since neither the bodies considered in this paper nor the freestream Mach number match the experimental data.

We consider the case of the ellipsoid with a 2:1 axes ratio described previously, assuming that the major axis of the ellipsoid is the radius of the experimental body $\frac{1}{4}$ in. The values of pressure and density behind the moving shock in the shock tube are the values at infinity in the present paper. For example, in the case of Fig. 8 of Davies' paper, $(\rho_\infty/p_\infty)^{1/2} = (0.86/a_0)$ where a_0 is the speed of sound at room temperature. With $r_0 = \frac{1}{4}$ in., a nondimensional time of the order of 1 (which is the value of T for the present case) represents a physical time of about 16.3 μsec. This result is in good agreement with the order of magnitude of the total time involved in the experiments, about 70 μsec. (Note that our computations are for $M_\infty = 3$, whereas the experiment is for M_∞ of the order of 1; moreover, our computations show only one part of the phenomenon to which the mentioned figure refers.)

Table 2 Total running times

A	15 sec	C	1.5 min
B	40 sec	D	6.0 min

References

[1] Hayes, W. D. and Probstein, R. F., *Hypersonic Flow Theory* (Academic Press Inc., New York, 1959), pp. 150–230.

[2] Belotserkovskii, O. M., "On the calculation of flow past axisymmetric bodies with detached shock waves using an electronic computing machine," Prikl. Mat. Mekh. **24**, 511 (1960).

[3] Moretti, G. and Abbett, M., "A fast, direct, and accurate technique for the blunt body problem," General Applied Science Labs., Westbury, N. Y., TR-583 (1966).

[4] Swigart, R. J., "A theory of asymmetric hypersonic blunt-body flows," AIAA J. **1**, 1034–1042 (1963).

[5] Vaglio-Laurin, R. and Ferri, A., "Theoretical investigation of the flow field about blunt-nosed bodies in supersonic flight," J. Aerospace Sci. **25**, 761–770 (1958).

[6] Van Dyke, M. D., "The supersonic blunt-body problem-review and extension," J. Aerospace Sci. **25**, 485–496 (1958).

[7] Garabedian, P. R. and Lieberstein, H. M., "On the numerical calculation of detached bow shock waves in hypersonic flow," J. Aerospace Sci. **25**, 109–118 (1958).

[8] Bohachevsky, I. O. and Rubin, E. L., "A direct method for computation of non-equilibrium flows with detached shock waves," AIAA J. **4**, 600–607 (1966).

[9] Godunov, S. K., Zabrodyn, A. W., and Prokopov, G. P., "A difference scheme for two-dimensional unsteady problems of gas dynamics and computation of flow with a detached shock wave," Zh. Vych. Mat. i Mat. Fiz. **1**, 1020 (1961).

[10] von Neumann, J. and Richtmyer, R., "A method for the numerical calculation of hydrodynamic shocks," J. Appl. Phys. **21**, 232 (1950).

[11] Lax, P. D. and Wendroff, B., "Difference schemes for hyperbolic equations with high order of accuracy," Commun. Pure Appl. Math. **17**, 381–398 (1964).

[12] Courant, R., Friedrichs, K. O., and Lewy, H., "Ueber die partiellen Differenzengleichungen der mathematischen Physik," Math. Ann. **100**, 32 (1928).

[13] Moretti, G., "Three-dimensional flow field analysis in reentry problems," *Sixth Symposium on Ballistic Missiles and Aerospace Technology* (Academic Press Inc., New York, 1961), Vol. IV, pp. 89–109.

[14] Moretti, G., "Three-dimensional supersonic flow computations," AIAA J. **1**, 2192–2193 (1963).

[15] Belotserkovskii, O. M., "Flow past a circular cylinder with a detached shock wave," Vychislitel'naia Mat. **3**, 149 (1958); also Avco TM RAD-9-TM-59-66 (1959).

[16] Perry, J., "A comparison of solutions to some blunt body problems," AIAA J. **8**, 1425–1426 (1966).

[17] Sedney, R. and Kahl, G. D., "Interferometric study of the blunt body problem," Ballistics Research Labs., Rept. 1100 (1960).

[18] Davies, L., "Bow-shock establishment and stagnation-point pressure measurements for a blunt-nosed body at supersonic speeds," Aeronautical Research Council London, Current Papers 776 (1965).

[19] Van Dyke, M. D. and Gordon, H. D., "Supersonic flow past a family of blunt axisymmetric bodies," NASA TR R-1 (1959).